Inelastic collisions of CaH with He at cryogenic temperatures

Vijay Singh, Kyle S. Hardman, Mei-Ju Lu, Aja A. Ellis, Muir J. Morrison, and Jonathan D. Weinstein[*]

Department of Physics, University of Nevada, Reno NV 89557, USA

(Dated: January 22, 2013)

Using helium buffer-gas cooling, we have prepared dense samples of ground-state molecular calcium monohydride (CaH $X^2\Sigma$) at cryogenic temperatures. We have used optical pumping to polarize the spin state of the CaH molecules and we have measured the inelastic collisions of molecular CaH with atomic helium at temperatures from 2 to 7 K. The measured CaH electronic spin depolarization rate coefficient increases rapidly with increasing temperature, increasing from 2×10^{-13} cm^3 s^{-1} to over 10^{-11} cm^3 s^{-1}. The strong dependence of rate coefficient on temperature is attributed to the CaH population in the first excited rotational state.

Keywords: cryogenic helium buffer gas cooling, cold molecules, optical pumping, spin polarization, cold collisions.

1. INTRODUCTION

Inelastic collisions change the internal states of the atoms and molecules. As interactions with external fields are state-dependent, inelastic collisions are of great importance for any experiment investigating the interaction of molecules with fields. In addition, inelastic collisions are of great consequence for sympathetic cooling of molecules with atoms [1–3], for quantum state control of chemical reactions [4–7], quantum computing with molecules [8], and experimental searches for the electric dipole moment of the electron using molecules [9, 10].

Inelastic collisions are also of great importance for magnetic trapping of molecules, as well as buffer-gas loading of magnetic traps. In the first experiment demonstrating buffer-gas loading of magnetic traps with molecules, Bretislav Friedrich and collaborators successfully trapped CaH at 0.4 K [11]. The success of this experiment depended on the nature of CaH–He collisions; specifically it required a large ratio of the elastic collision cross-section to the cross-section for collisions that change the Zeeman state (i.e. spin state) of the molecule. The inelastic cross-section was found to be extremely small: at 0.4 K, the $X^2\Sigma(v''=0)$ ground state of CaH has a rate coefficient of $k = 10^{-17\pm1}$ cm^3/s for inelastic spin-changing collisions with ^{3}He [11–13].

Subsequent theoretical work explained the physics of spin-changing collisions in $^2\Sigma$ molecules [14–16]. For molecules in the $N''=0$ rotational state, the electronic spin depolarization occurs predominantly through mixing of the $N''=0$ and $N''=1$ states during a collision; the spin-rotation coupling of the $N''=1$ state then allows for spin-changing collisions. The cross-section of this process is expected to scale as γ_{sr}^2/B^4, where γ_{sr} is the spin rotation coupling constant and B is the rotational constant [13, 15]. In CaH, the rotational splitting ($B = 4.277$ cm^{-1}) is large compared to the spin rotation coupling constant ($\gamma_{sr} = 0.0415$ cm^{-1}). Consequently, CaH

spin depolarization in the $N''=0$ rotational state occurs with a cross-section many orders of magnitude smaller than the elastic collision cross-section [11].

In subsequent work measuring inelastic collisions of CaF $X^2\Sigma(v''=0, N''=0)$ molecules with ^{3}He at 2 K, a much larger inelastic rate coefficient was measured, with Zeeman relaxation collisions occurring with a rate coefficient of $k = (7.7 + 5.4/-2.5) \times 10^{-15}$ cm^3/s, despite CaF's low value of γ_{sr} [13]. This large value of Γ_Z was attributed to the transfer of CaF population between the ground and the first excited rotational states which occurs in thermal equilibrium at 2 K. In excited rotational states, spin changing collisions occur through the spin rotation coupling and are expected to have a large cross-section [13]. The rate coefficient for rotation-changing collisions is generally expected to be large [14]; consequently one would expect — at sufficiently high temperatures — the population in the excited rotational state would mediate Zeeman relaxation in the ground rotational state population.

If rotation-changing collisions are sufficiently fast, one would expect the Zeeman relaxation rate coefficient for the ground rotational state to have the form

$$k = \frac{1}{Z} \sum_{i=0,1,\ldots} \Gamma_i g_i e^{-E_i/k_B T} \qquad (1)$$

where T is the temperature, Z is the partition function, Γ_i is the Zeeman relaxation rate coefficient of the ith rotational state, and g_i and E_i are the degeneracy and energy of that state, respectively. As we expect $\Gamma_{i\neq0} \gg \Gamma_0$, this rate coefficient should exhibit a very strong temperature dependence at temperatures comparable to the energy difference between the ground and first excited state.

Isolated data points with different molecules have been shown to conform to this model [11, 13]; herein we further test the model by measuring the spin depolarization rate of a single species as a function of temperature, measuring CaH collisions with ^{4}He atoms from 2 to 7 K.

2. EXPERIMENT

We produce cold molecular CaH by cryogenic helium buffer gas cooling [17]. The experiment takes place in a 10 cm cubic copper cell, as described in references [18] and [5]. For high-temperature data ($\gtrsim$ 5 K) the cell is cooled by a commercial pulse tube cooler [18]. For the low-temperature data ($\lesssim$ 5 K) the cell is cryogenically cooled by a cryogen-free pumped-^{4}He refrigerator, which uses a commercial pulse tube cooler to condense the circulating ^{4}He [5, 19]. The cell temperature is monitored by a ruthenium oxide resistor. The helium density is determined from a room-temperature pressure gauge connected to the cryogenic cell through a thin tube. We correct for the thermomolecular pressure ratio with the Weber-Schmidt equation [20]. The uncertainty in measured helium densities in this paper is approximately $\pm 20\%$. Gas-phase CaH molecules are produced by laser ablation of a solid target of 95% pure CaH_2 using a frequency-doubled pulsed Nd:YAG laser.

The ground state CaH molecules are detected on the $B\ ^2\Sigma(v'=0, N'=1, J'=\frac{1}{2}) \leftarrow X\ ^2\Sigma(v''=0, N''=0, J''=\frac{1}{2})$ transition at 634 nm [21, 22], using laser absorption spectroscopy. Typical probe powers are on the order of a few μW, with a beam diameter of a few mm [23]. The CaH population is monitored in terms of optical density (OD), with the definition that the transmission $T \equiv e^{-\mathrm{OD}}$. From our measured OD, we determine that we are able to produce CaH densities as high as $n_{\mathrm{CaH}} = 10^8$ cm^{-3}, with ablation energies of tens of mJ [24].

The translational temperature of the CaH molecules is measured through absorption spectroscopy, and determined from the Doppler broadening of the transition. Unfortunately, this technique is of limited sensitivity below 3 K in our apparatus. Consequently, to measure temperatures below 3 K, we ablate atomic lithium under the same experimental conditions, and measure the temperature from the Doppler broadening of the ^{6}Li absorption spectrum. Under our experimental conditions Doppler broadening is the dominant broadening mechanism, and thermalization with the buffer-gas is expected to occur within 1 ms.

3. MEASUREMENT OF INELASTIC COLLISIONS

We polarize the spin state of the CaH molecules using optical pumping. The optical pumping setup is shown in Fig. 1. We use a pair of Helmholtz coils to generate a magnetic field of $\sim$ 5 Gauss to split the degeneracies of the spin states and define a polarization axis. Under our experimental conditions, the temperature is very large compared to the Zeeman splitting. In thermal equilibrium, the sample is essentially unpolarized.

To induce a polarization, we optically pump the molecules with a pulse of circularly polarized (σ^+) light
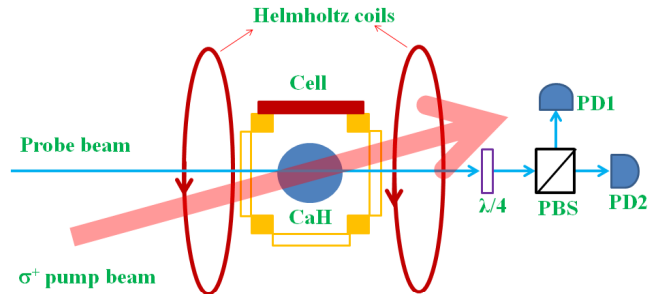

FIG. 1. (color online). Experimental setup for the electronic spin polarization of the CaH, as described in the text. The angle between pump and probe beams is exaggerated for clarity.

along the magnetic field to optically pump the Zeeman sub-levels ($m_F'' = +1$) of the hyperfine states of the CaH [25]. Typical pump laser beam powers are $\sim$ 2.5 mW, and the pumping beam is turned on and off using a mechanical shutter. The CaH energy levels are shown in Fig. 2. The σ^+ pump laser is tuned on resonance with the $F' = 1 \leftarrow F'' = 1$ transition to pump the CaH molecules into the $m_F'' = +1$ dark state.

We measure the CaH spin polarization using a 3.5 μW linearly polarized probe laser beam on resonance with the $F' = 1 \leftarrow F'' = 1$ transition as shown in Fig 2. A quarter wave ($\frac{\lambda}{4}$) plate and a polarizing beam splitter (PBS) after the cryogenic cell separate the σ^+ and σ^- components of the probe light for detection on photodetectors PD1 and PD2, respectively.

The measured OD's for the σ^+ and σ^- components of the probe beam are shown as a function of time in Fig. 3. During optical pumping, the CaH OD for σ^+ decreases because of optical pumping of the CaH molecules into the dark state. When the optical pumping beam is turned off, the CaH population starts to return to the thermal equilibrium due to collisions of the CaH molecules with ^{4}He buffer gas atoms [13, 15]. In thermal equilibrium the populations of the m_F'' levels are very nearly equal, and the OD for σ^+ light becomes nearly equal to that for σ^- light.

To measure the CaH electronic spin depolarization rate, we calculate the ratio of the OD's of σ^+ and σ^- light as a function of time after optical pumping, and fit it to $A \cdot e^{-t/\tau} + B$ (where t is the time and A and B are constants). This fit is shown in Fig. 4. We define the exponential constant $1/\tau$ as the electronic spin depolarization rate.

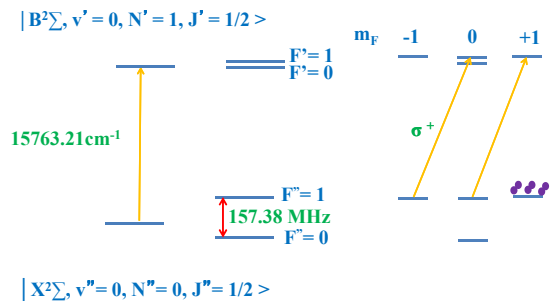In order to confirm that the spin depolarization is due to collisions with ^{4}He buffer gas, we have mea-

FIG. 2. (color online). Transitions used to prepare and detect the electronic spin polarization of CaH [21, 22, 26]. The small dumbbells represent the $F''=1$ molecules pumped into the $m''_F = +1$ dark state. **Both pump and probe beams are taken from a grating stabilized diode laser. The exited electronic(B $^2\Sigma$) state lifetime is 58.1$\pm$1.9 ns** [24].
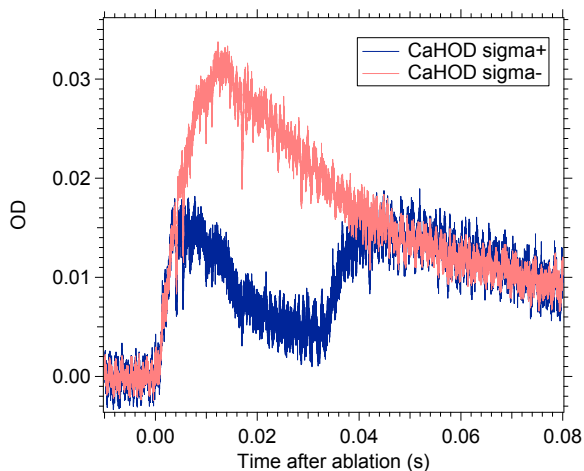

FIG. 4. (color online). Temporal evolution of ratio of the CaH ODs for σ^+ and σ^- light from a linearly polarized probe at a helium density of 1.2×10^{15} cm^{-3} and a CaH temperature of 2 K.

FIG. 3. (color online). The CaH OD for σ^+ and σ^- light. The ablation laser is fired at $t=0$. The data is taken at a helium density of 1.2×10^{15} cm^{-3} and a CaH temperature of 2 K. The shutter which controls the optical pumping beam was open from 3 to 31 ms; the shutter takes 3 ms to fully open and 1.2 ms to fully close.

FIG. 5. (color online). A plot of the CaH spin depolarization rate $(1/\tau)$ versus n_{He}. The data is taken at a temperature of 2.5 ± 0.2 K and a constant ablation energy of 12 mJ. The CaH spin depolarization rate increases linearly with increase in n_{He}, as expected for CaH inelastic collisions with ^{4}He.

sured the depolarization rate at ^{4}He densities (n_{He}) from 1.2×10^{-15} to 6×10^{-15} cm^{-3}. A plot of the CaH spin depolarization rate as a function of n_{He} is shown in Fig. 5. The CaH spin depolarization rate increases linearly with increase in n_{He}, as expected for inelastic collisions with ^{4}He. We note that there are small deviations from this linear dependence at low density; this is likely due
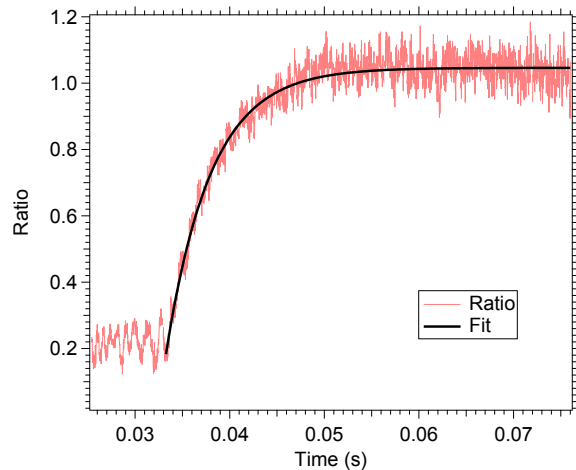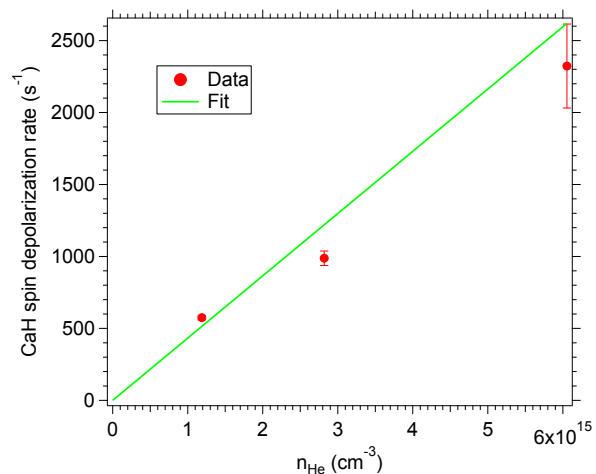
to diffusion of molecules in and out of the pump beam region [27].

From the CaH depolarization data, we calculate the CaH spin depolarization rate coefficient $k \equiv 1/(\tau \cdot n_{\mathrm{He}})$. We have measured the CaH spin depolarization rate at temperatures ranging from 2 to 7 K. The measurements are plotted in Fig. 6. The CaH spin depolarization rate coefficient shows a strong temperature dependence, varying over two orders of magnitude over this small temperature range. We note that even at 2 K the CaH spin depolarization rate coefficient is still very large compared
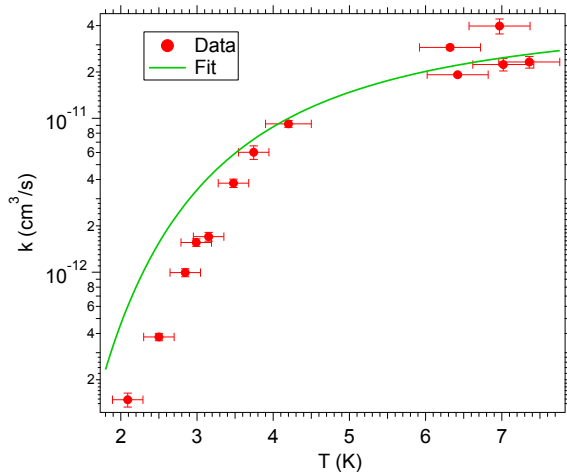
FIG. 6. (color online). The CaH spin depolarization rate coefficient (k) as a function of temperature. Going down in temperature from 7 K to 2 K, the CaH rate coefficient is reduced by two orders in magnitude. This strong dependence of spin depolarization rate on temperature is attributed to the CaH population in exited rotational states.
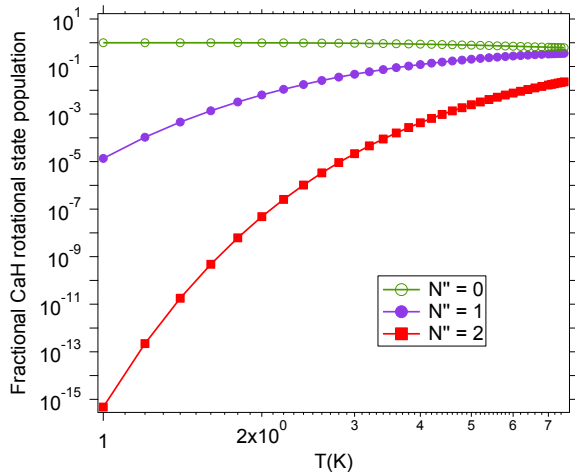

FIG. 7. (color online). Calculated fractions of population of the ground, first excited, and second excited rotational states of CaH (in thermal equilibrium) as a function of temperature. In our temperature range (2 to 7 K) of measuring CaH–^{4}He inelastic collisions, CaH population is predominantly distributed over the ground ($N'' = 0$) and first excited ($N'' = 1$) rotational states.

to its value at 0.4 K [11].

In thermal equilibrium, the CaH population in an excited rotational state (P_e) relative to ground rotational state population (P_g) is given by

$$\frac{P_e}{P_g} = \frac{2 \cdot N_e'' + 1}{2 \cdot N_g'' + 1} \cdot \exp\left(-\frac{\Delta E_{rot}}{k_B T}\right) \qquad (2)$$

where ΔE_{rot} is the energy splitting between excited (N_e'') and ground rotational (N_g'') states. The factor $\frac{2 \cdot N_e'' + 1}{2 \cdot N_g'' + 1}$ accounts for the relative degeneracies of the excited and ground rotational levels.

The rotational constant (B) of the $v'' = 0$ vibrational state of $^2\Sigma$ electronic state of the CaH is 4.277 cm^{-1} [28]. The calculated fractions of CaH population in ground ($N'' = 0$), first exited ($N'' = 1$), and second excited ($N'' = 2$) rotational states as a function of temperature are shown in Fig. 7. The population of excited rotational states decreases exponentially with decrease in CaH temperature and therefore the CaH spin depolarization rate decreases exponentially with decrease in temperature, as shown in Fig. 6.

We note that at higher temperatures, we are able to directly measure the CaH population in the ground ($N'' = 0$) and first exited ($N'' = 1$) rotational states, and the rotational populations are consistent with being in thermal equilibrium with the translational temperature. At lower temperatures the CaH population in $N'' = 1$ state is too small to detect spectroscopically.

4. SPIN DEPOLARIZATION RATE COEFFICIENTS FOR EXCITED ROTATIONAL STATES

Following Maussang *et. al.* [13], we model the CaH electronic spin changing collision rate coefficient for the ground rotational state of CaH as follows:

$$k = \frac{3A \cdot e^{-\frac{12.3\ K}{T}}}{1 + 3 \cdot e^{-\frac{12.3\ K}{T}}} \qquad (3)$$

Fig. 6 shows our data fit to the functional form of Equation 3, with A as the single free parameter in the fit.

Equation 3 is obtained using the fact that the spin depolarization rate coefficient in the measured temperature range is dominated by the CaH population in exited rotational states [13]. We restrict our model to the first excited rotational state ($N'' = 1$). As seen in Fig. 7, in our temperature range the CaH population in higher rotational states ($N'' > 1$) is sufficiently small compared to that in $N'' \leq 1$ rotational states that it is not expected to make a significant contribution. The factor 12.3 K is the energy splitting of $N'' = 0$ and $N'' = 1$ rotational states of the CaH expressed as a temperature.

From the fit we have determined $A = (7.2 \pm 1.8) \times 10^{-11}$ cm^3/s. The uncertainty in our measurement of this factor is dominated by the uncertainty in the helium density.

We note that the rate coefficient A would be expected to be equal to the electronic spin depolarization rate coefficient of the $N'' = 1$ state in the limit that rotation-changing collisions are very fast compared to spin-changing collisions. Due to the large value of the

rate coefficient, this is unlikely to be the case; this value is within an order of magnitude of the Langevin rate coefficient for CaH–^{4}He collisions [1, 29–32].

We observe that including spin depolarization from the ground state in Equation 3 does not significantly improve the fit, and the ground state rate coefficient from the fit is consistent with zero. Prior measurements indicate that the ground state rate coefficient is on the order of 10^{-17} cm^3/s [13], which is negligible compared to the measured rate coefficients reported here.

from 2 to 7 K. The spin depolarization rate coefficient shows a strong dependence on temperature. This strong temperature dependence is in excellent qualitative agreement with a simple model that attributes the relaxation to the CaH population in first excited rotational state [13]. We note that there are deviations between the data and the model; this is not surprising, as collisional cross-sections for individual rotational states (for both rotation-changing collisions and spin-changing collisions) are expected to change over this temperature range [14, 15].

5. CONCLUSIONS

We have measured electronic spin depolarization rate coefficient of the CaH molecules in a temperature range

ACKNOWLEDGEMENTS

[1] M. Lara, J. L. Bohn, D. Potter, P. Soldán, and J. M. Hutson, Phys. Rev. Lett. **97**, 183201 (2006).

[2] M. T. Hummon, T. V. Tscherbul, J. Kłos, H.-I. Lu, E. Tsikata, W. C. Campbell, A. Dalgarno, and J. M. Doyle, Phys. Rev. Lett. **106**, 053201 (2011).

[3] T. V. Tscherbul, J. Klos, and A. A. Buchachenko, Phys. Rev. A **84**, 040701(R) (2011).

[4] S. Ospelkaus, K.-K. Ni, D. Wang, M. H. G. de Miranda, B. Neyenhuis, G. Quéméner, P. S. Julienne, J. L. Bohn, D. S. Jin, and J. Ye, Science **327**, 853 (2010), http://www.sciencemag.org/content/327/5967/853.full.pdf.

[5] V. Singh, K. S. Hardman, N. Tariq, M.-J. Lu, A. Ellis, M. J. Morrison, and J. D. Weinstein, Phys. Rev. Lett. **108**, 203201 (2012).

[6] T. V. Tscherbul and R. V. Krems, Phys. Rev. Lett. **97**, 083201 (2006).

[7] R. V. Krems, Phys. Chem. Chem. Phys. **10**, 4079 (2008).

[8] D. DeMille, Phys. Rev. Lett. **88**, 067901 (2002).

[9] A. C. Vutha, W. C. Campbell, Y. V. Gurevich, N. R. Hutzler, M. Parsons, D. Patterson, E. Petrik, B. Spaun, J. M. Doyle, G. Gabrielse, and D. DeMille, Journal of Physics B: Atomic, Molecular and Optical Physics **44**, 079803 (2011).

[10] J. J. Hudson, D. M. Kara, I. J. Smallman, B. E. Sauer, M. R. Tarbutt, and E. A. Hinds, Nature **473**, 493 (2011).

[11] J. D. Weinstein, R. deCarvalho, T. Guillet, B. Friedrich, and J. M. Doyle, Nature **395**, 148 (1998).

[12] J. D. Weinstein, *Magnetic trapping of atomic chromium and molecular calcium monohydride*, Ph.D. thesis, Harvard University (2001).

[13] K. Maussang, D. Egorov, J. Helton, S. Nguyen, and J. Doyle, Physical Review Letters **94**, 123002 (2005).

[14] N. Balakrishnan, G. C. Groenenboom, R. V. Krems, and A. Dalgarno, Journal of Chemical Physics **118**, 7386 (2003).

[15] R. V. Krems, A. Dalgarno, N. Balakrishnan, and G. C. Groenenboom, Phys. Rev. A **67**, 060703 (2003).

[16] R. V. Krems and A. Dalgarno, Journal of Chemical Physics **120**, 2296 (2004).

[17] W. C. Campbell and J. M. Doyle, in *Cold Polar Molecules: Creation and Applications*, edited by R. V. Krems, J. M. Doyle, B. Friedrich, and G. Meijer (CRC, 2009).

[18] M.-J. Lu, K. S. Hardman, J. D. Weinstein, and B. Zygelman, Phys. Rev. A **77**, 060701(R) (2008).

[19] K. S. Hardman, *Closed Cycle Liquid 4He Cryogenic Cooler: Toward controlling chemical reactions*, Master's thesis, University of Nevada, Reno (2011).

[20] T. R. Roberts and S. G. Sydoriak, Physical Review **102**, 304 (1956).

[21] T. C. Steimle, J. Gengler, and J. Chen, Canadian Journal of Chemistry **82**, 779 (2004), http://www.nrcresearchpress.com/doi/pdf/10.1139/v04-077.

[22] L.-E. Berg and L. Klynning, Astron. Astrophys. Suppl. **13**, 325 (1974).

[23] V. Singh, *Chemical Reactions of Li and CaH and Inelstic Ti-Ti Collisions at Cryogenic Temperatures.*, Ph.D. thesis, University of Nevada Reno (2012).

[24] L.-E. Berg, K. Ekvall, and S. Kelly, Chemical Physics Letters **257**, 351 (1996).

[25] M. Auzinsh, D. Budker, and S. M. Rochester, *Optically Polarized Atoms* (Oxford University Press, New York, 2010).

[26] W. L. Barclay, M. A. J. Anderson, and L. M. Ziurys, The Astrophysical Journal **408**, L65 (1993).

[27] M.-J. Lu and J. D. Weinstein, New Journal of Physics **11**, 055015 (2009).

[28] K.P. Huber and G. Herzberg, "Constants of Diatomic Molecules" (data prepared by J.W. Gallagher and R.D. Johnson, III) in NIST Chemistry WebBook, NIST Standard Reference Database Number 69, Eds. P.J. Linstrom and W.G. Mallard, National Institute of Standards and Technology, Gaithersburg MD, 20899, http://webbook.nist.gov, (retrieved November 29, 2012).

[29] A. J. Stone, *Theory of Intermolecular Forces* (Oxford University Press, Oxford, 1997).

[30] M. Masili and A. F. Starace, Phys. Rev. A **68**, 012508 (2003).

[31] C. I. Frum, J. J. Oh, E. A. Cohen, and H. M. Pickett., The Astrophysical Journal **408**, L61 (1993).

[32] J. Chen and T. C. Steimle, The Journal of Chemical Physics **128**, 144312 (2008).